

Using phosphorus doping of MoO₃/ZSM-5 to modify performance in methane dehydroaromatisation

S. Burns^a, J.S.J. Hargreaves^{a,*}, P. Pal^b, K.M. Parida^c, S. Parija^c

^a WestCHEM, Department of Chemistry, Joseph Black Building,
University of Glasgow, Glasgow G12 8QQ, UK

^b Refining Technology Division, Indian Institute of Petroleum, Council for Scientific and Industrial Research,
Haridwar Road, Mohkampur, Dehra-Dun 248005, India

^c Regional Research Laboratory, Council for Scientific and Industrial Research,
Bhubaneswar 751 013, Orissa, India

Received 1 September 2005; received in revised form 28 September 2005; accepted 28 September 2005

Available online 3 November 2005

Abstract

The performance of methane dehydroaromatisation catalysts prepared by the impregnation of H-ZSM-5 with ammonium heptamolybdate and phosphomolybdic acid precursors has been found to be different. Particular attention has been paid to hydrogen production which, although the major gas-phase product of dehydroaromatisation, is generally not reported. The use of phosphomolybdate leads to lower activity catalysts. When 5 wt.% of phosphorus is added to the catalyst prepared from ammonium heptamolybdate, the activity is suppressed and H₂ is seen as the sole gas-phase product. The rate of hydrogen formation increases with time on stream passing through a maximum, which is associated with the loss of an inorganic phosphite phase from the catalyst. Bulk MoO₃ and P doped MoO₃ samples are observed to produce H₂ as a result of carburisation. Although the general pattern of hydrogen formation is similar to the 5 wt.% doped zeolite catalyst, in these cases gas-phase carbon oxides are also associated with the hydrogen maximum.

© 2005 Elsevier B.V. All rights reserved.

Keywords: Methane; Dehydroaromatisation; Hydrogen; Benzene; Molybdenum oxide; Molybdenum carbide; ZSM-5

1. Introduction

The direct catalytic conversion of methane into higher added value chemicals is an area of immense interest, e.g. [1,2]. This is a consequence of the high relative abundance of methane, although its stability makes any conversion process challenging. Amongst the strategies employed to date have been the use of a gas-phase oxidant such as O₂ and N₂O in oxidative coupling to produce higher hydrocarbons [3] or oxygenates such as methanol and formaldehyde [4]. Generally these approaches have proved unsuccessful due to the much greater susceptibility of the products to gas-phase oxidation than methane and limitations of gas-phase free radical chemistry. As a consequence, alternative strategies have sought to develop routes to the conversion of methane in the absence of gas-phase oxidants. Amongst

these routes, the two step homologation of methane has attracted interest wherein methane is initially dehydrogenated on a metal surface and the deposited carbonaceous species are subsequently re-hydrogenated to yield higher hydrocarbons either isothermally [5] or using a dual temperature cycle [6]. Another pathway which has attracted considerable attention is the dehydroaromatisation of methane [7] to produce aromatics, primarily benzene, and hydrogen. This reaction, which is generally run at ambient pressure and temperatures of 700 °C or above, is equilibrium limited with the limit of conversion being 11.5% at atmospheric pressure and 700 °C [8]. Whilst a wide range of catalysts have been screened for this reaction, MoO₃/ZSM-5 is the most well studied and amongst the most active. However, even with this system activities have been low with low space velocities being required for conversion approaching equilibrium. Catalysts have also been observed to suffer relatively rapid deactivation, which has been attributed to coke formation. Accordingly, a number of strategies have been adopted to enhance activity and/or suppress deactivation. These have included the addition of metal ion

* Corresponding author.

E-mail address: justinh@chem.gla.ac.uk (J.S.J. Hargreaves).

dopants such as Co^{2+} and Fe^{3+} [9,10] and also the inclusion of low levels of gas-phase species such as CO and CO_2 [10–12] in the feedstream. The active form of the catalyst is still uncertain, but there has been general agreement that the active phase of the molybdenum is the carbide [13–15] during reaction. Studies aimed at elucidating structure-sensitivity have proposed that the face centred-cubic MoC_{1-x} phase is more active than the hexagonal $\beta\text{-Mo}_2\text{C}$ phase [16,17]. As regards the mechanism, there is a general consensus that methane is initially dehydrogenated to form ethylene (which is observed to be a major by-product of reaction), which is then cyclised to form benzene, e.g. [18]. Acetylene has also been proposed to be a key-intermediate [19]. In addition to benzene, a range of additional hydrocarbons is produced with C_2 hydrocarbons (particularly ethylene) being the most significant, but reports of toluene, naphthalene and even heavier aromatics have been made, e.g. [10].

In this manuscript the effect of phosphorus doping on the activity of $\text{MoO}_3/\text{ZSM-5}$ based dehydroaromatisation catalysts is investigated. Within the literature, the inclusion of phosphate in different dehydroaromatisation catalysts has been shown to cause different effects dependent upon its form. When phosphate is incorporated as a framework species in the zeolite host, it has been reported to enhance the production of aromatics, which has been ascribed to a modification in acidity [20,21]. However, when added to $\text{MoO}_3/\text{ZSM-5}$ as a dopant by impregnation with phosphoric acid it was observed to lower, but not eliminate, benzene production [22]. In the study reported here, phosphorus has been added in different forms—simultaneously with the active molybdenum component in the form of phosphomolybdic acid and, at higher levels, by impregnation of $\text{MoO}_3/\text{ZSM-5}$ with ammonium hydrogen phosphate. Phosphomolybdic acid is a potentially interesting precursor for several reasons. Unlike methods relying on the post-preparative doping of $\text{MoO}_3/\text{ZSM-5}$, its use ensures that the Mo and P components are added in a single chemical unit, which implies that there may be a potentially more direct association of phosphorus with the active molybdenum component. Secondly, in a temperature programmed carburising study utilising a CH_4/H_2 mixture, Perez-Romo et al. [23] have shown that, in contrast to MoO_3 , the use of phosphomolybdic acid as precursor eliminates the formation of coke associated with the Mo_2C phase. The presence of phosphorus was also reported to induce carburisation at lower temperature. Particular attention has also been paid to the effects of phosphate addition on the production of hydrogen. Despite the fact that hydrogen is expected to be the major product of reaction, very few studies in the literature have reported its quantification. This is especially surprising in view of the fact that the production of hydrogen is at least of comparable, and probably greater, interest to that of benzene by this pathway. The dehydroaromatisation reaction could be viewed as a potential alternative route to hydrogen production from methane. Direct decomposition of methane to produce CO-free sources of hydrogen for use as chemical feedstocks in reactions such as ammonia synthesis and/or for fuel cell applications have been the subject of some interest, e.g. [24–26]. The catalysts generally employed are supported metals such as nickel and generally catalyst deactivation is an issue.

2. Experimental

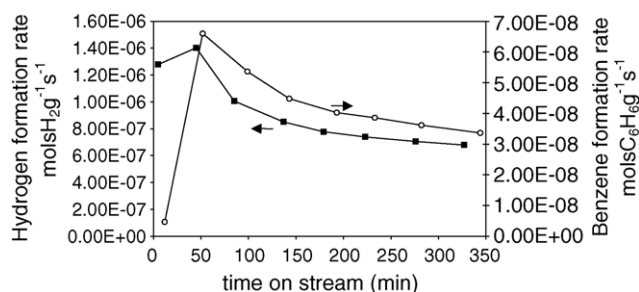
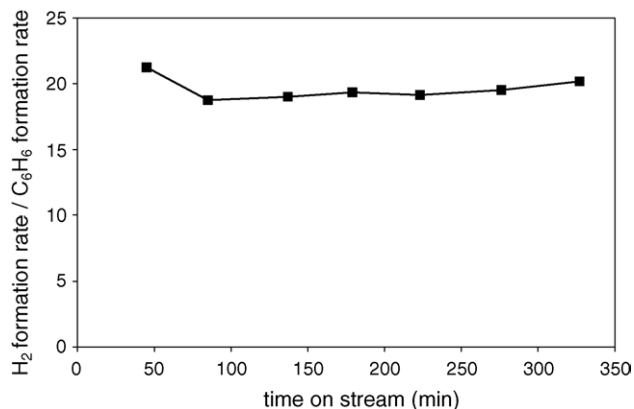
Phosphorus doped samples were prepared by impregnation of a H-ZSM-5 (Si/Al = 50, Zeolyst) with an aqueous solution of phosphomolybdic acid to achieve a 5 wt.% loading of MoO_3 , followed by drying at 80°C for 24 h and calcining in air at 500°C for a further 16 h. For reference, a non-phosphorus containing 5 wt.% $\text{MoO}_3/\text{ZSM-5}$ was prepared by an analogous procedure using an aqueous solution of ammonium heptamolybdate. This catalyst is denoted 5% $\text{MoO}_3/\text{ZSM-5}$. Phosphorus doping of this reference catalyst was also performed to achieve a 5 wt.% P level by the addition of an aqueous ammonium dihydrogen phosphate solution followed by drying and calcination as described above. This catalyst is denoted 5 wt.% P/5 wt.% $\text{MoO}_3/\text{ZSM-5}$ and was light blue in colour. Unsupported 5 wt.% P/ MoO_3 was prepared by the addition of an aqueous solution of ammonium dihydrogen phosphate to bulk ammonium heptamolybdate, followed by drying at 80°C for 24 h and calcining in air at 500°C for a further 16 h.

Catalyst testing was performed in a fixed bed silica glass microreactor wherein 0.5 g of catalyst in powder form was held centrally within a tube furnace between silica wool plugs. Methane (BOC 99.5%) was flowed over the catalyst at 8 ml min^{-1} and nitrogen (2 ml min^{-1}) was used as an internal standard. The reaction was performed at 700°C , which was measured using a thermocouple attached to the outer wall of the reactor tube. Product analysis was performed on a HP 5890 GC using a combination of FID and TCD with a Poraplot Q column and a Molecular Sieve 13X column respectively. Where applicable, CO and CO_2 concentrations were monitored by off-line FT-IR spectroscopy of the reactor effluent stream, which was continuously passed through a flow cell directly attached to the reactor exit. In the following, reaction data is reported in terms of mass normalised rates of formation of products rather than conversion and selectivity data. This approach has been adopted because, at the generally low levels of conversion which occur, the measurement of a small difference in the GC data may be subject to a relatively large degree of error. This is a particular concern given that the reaction never attains steady state—it is either activating or deactivating. Within the literature, expressing data for this reaction as formation rates is fairly common practice, e.g. [11,12].

CHN analysis was performed using a CE-440 Elemental Analyser.

Laser Raman Spectroscopy was performed with powder specimens of 5 and 15 wt.% phosphomolybdic acid/H-ZSM-5 catalysts. The samples were in the fresh/calcined form. A Renishaw Ramascope 2000 spectrometer, which consisted of an integral microscope, a notch filter, single grating and a cooled CCD detector was used. The spectral range examined was in the region of $400\text{--}1400\text{ cm}^{-1}$ and multiple analyses were performed on each sample. Excitation at 632.8 nm was delivered by a Spectra Physics 2020 helium–neon laser source (40 mW).

Powder diffraction studies were performed on a Siemens D5000 instrument using $\text{Cu K}\alpha$ radiation in the 2θ range $5\text{--}75^\circ$ using a step size of 0.02° and a counting rate of 1.5 s/step . Samples were prepared by compaction into silicon sample holders.

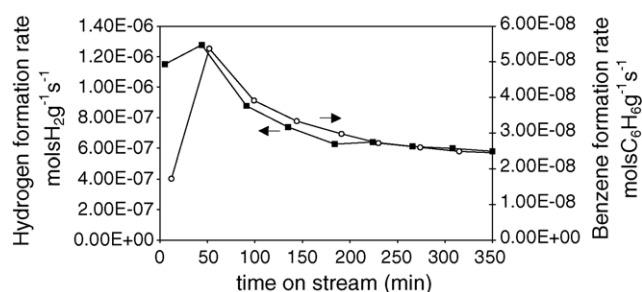
Fig. 1. Benzene and hydrogen formation rates of 5 wt.% MoO₃/ZSM-5.Fig. 2. Ratio of hydrogen to benzene formation rate as a function of time on stream for 5 wt.% MoO₃/ZSM-5.

3. Results and discussion

Fig. 1 presents the benzene and hydrogen formation rates for the 5 wt.% MoO₃/ZSM-5 catalyst which was run at 700 °C for 6.5 h. The general form of the benzene profile is comparable to others reported in the literature in that there is an initial induction period after which the rate of formation declines with time on stream. In general terms, the hydrogen formation profile is similar to that for benzene except that the induction period is less pronounced. If benzene were the sole carbon containing product produced, the ratio of hydrogen to benzene formation rates would be expected to be 9, however it is in fact ca. 18 as shown in Fig. 2. This is indicative of the production of other higher hydrocarbons, as reported by others, e.g. [10] and coke deposition. The formation of a yellow deposit of polyaromatic species is consistently observed whenever, and only whenever, benzene is produced in the experiments described. These high boiling point compounds have not been quantified. The results of post-reaction CHN analysis presented in Table 1 lead to the

Table 1
CHN analysis post-reactor materials

Sample	%C	%H	%N
5 wt.% MoO ₃ /ZSM-5	5.70	0.11	–
5 wt.% P/5 wt.% MoO ₃ /ZSM-5	0.22	–	–
5 wt.% P/MoO ₃	5.71	–	–
5 wt.% MoO ₃ /ZSM-5 prepared from phosphomolybdic acid	5.67	0.22	–

Fig. 3. Benzene and hydrogen formation rates of 5 wt.% MoO₃/ZSM-5 prepared from phosphomolybdic acid.

conclusion that the major contribution to hydrogen formation is from coke formation. If the stoichiometry of the molybdenum containing phase is assumed as Mo₂C, as is often proposed in the literature, e.g. [14], the amount of contribution of carbidic carbon would be 0.21 wt.% meaning that ca. 5.49 wt.% carbon is deposited as coke. The relative constancy of the ratio between hydrogen and benzene during the reaction run is interesting, since this demonstrates that they decline at similar rates. Fig. 3 presents formation rate data for the 5 wt.% MoO₃/ZSM-5 catalyst prepared from a phosphomolybdic acid precursor (the P/Mo molar ratio is dictated by the formula of the Keggin unit, [PMo₁₂O₄₀]³⁻, and is therefore 0.08). In comparison to Fig. 1, it is apparent that the inclusion of a very low level of phosphorus dopant has produced a decrease in the benzene and hydrogen production rates. The hydrogen to benzene formation rate ratio appears to be slightly higher than that for the non-phosphorus containing catalyst, suggesting that the benzene selectivity is lowered with respect to that for hydrogen. A possible explanation for this effect may be enhanced coking which may be the result of the modified acidity of the catalyst. The carbon data in Table 1 is consistent with this, since although the overall conversion is suppressed in the case of phosphorus addition, the level of coke is comparable. The effects of phosphorus on the acidity are likely to be dependent upon the level of incorporation and the nature of the phase with which it is associated. For example, phosphorus modification of MoO₃ is known to enhance acidity [27], whereas in ZSM-5 it has been reported to decrease total acidity by, in particular, removal of the strongest acid sites [28]. Again, the relative constancy of the ratio suggests that the rate of decline in the benzene and hydrogen formation rates is similar. Considering the low levels of phosphorus addition, the effects on catalytic performance are comparatively dramatic. There are a number of possible explanations for this. One possibility is that the dispersions of the active phases of molybdenum differs between catalysts, which may be anticipated in view of the fact that the impregnating ion is Mo₇O₂₄⁶⁻ in one case and [PMo₁₂O₄₀]³⁻ in the other. Re-dispersion of oxomolybdenum species has been reported to occur on calcination [13] and so this may be expected to be of limited significance. The thermal decomposition of phosphomolybdic acid supported on silica has also been shown to proceed via the metastable β-MoO₃ phase [29], which may have different carbiding characteristics than those for the more usual phase. However, this phase has only been observed to be stable at lower temperatures than those

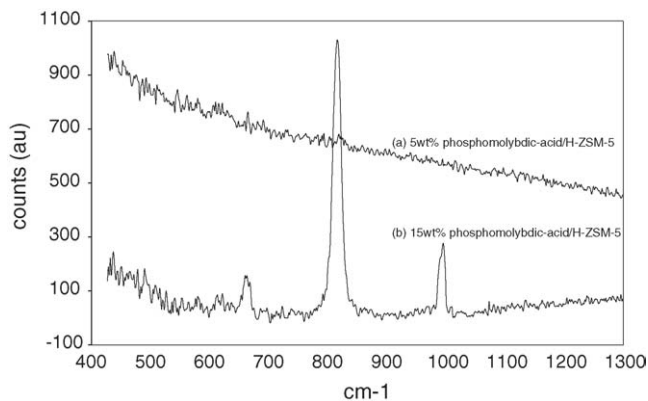


Fig. 4. Raman spectra of calcined $\text{MoO}_3/\text{ZSM-5}$ prepared from phosphomolybdic acid (a) 5 wt.% and (b) 15 wt.%.

employed in the calcination and reaction procedures used in this study, and temperature programmed carbidation studies of bulk phosphomolybdic acid have been reported to produce the expected hexagonal $\beta\text{-Mo}_2\text{C}$ polymorph [23]. In the case of silica as a support, calcination at 500°C was reported to completely transform $\beta\text{-MoO}_3$ into $\alpha\text{-MoO}_3$. However, the possibility that the metastable $\beta\text{-MoO}_3$ is stabilised to higher temperatures cannot be ruled out. In powder X-ray diffraction studies performed on pre- and post-reaction catalysts prepared from both precursors, only reflections which can be indexed to the ZSM-5 framework are apparent, implying that the molybdenum dispersion is high in each case. Accordingly, Raman spectroscopy has been applied to the pre-reaction catalysts and the results are shown in Fig. 4. It is apparent that the bands at ca. 820 and 995 cm^{-1} which would be expected for the Mo–O–Mo and Mo=O stretches of $\alpha\text{-MoO}_3$ [30] do not occur, and it is only at much higher loadings such as 15 wt.% that these features appear (Fig. 4(b)); albeit inhomogeneously as they were not observed in every sampling point. Nor is evidence for $\beta\text{-MoO}_3$ observed in either case, bands for this species would be expected to occur at around 770 , 850 and 900 cm^{-1} [31]. Therefore, the catalyst precursor cannot be considered as $\text{MoO}_3/\text{ZSM-5}$, which is the way in which it is sometimes designated. However, for example, in Mo EXAFS experiments, Zhang et al. [14] have reported that the radial distribution function of calcined catalyst precursors prepared from ammonium heptamolybdate is completely different from MoO_3 . Wang et al. [13] have shown that small crystallites of ammonium heptamolybdate are present on the external surface of ZSM-5 following impregnation and drying. After calcination, molybdenum oxide species were proposed to disperse themselves non-uniformly on the external surface of ZSM-5, with some species entering the channel structure and modifying acidity. Iglesia et al. [32,33] have proposed that the precursor form of Mo in their catalysts, which were prepared via a stepped temperature programmed heating of a physical mixture of ZSM-5 and MoO_3 , was $\text{Mo}_2\text{O}_5^{2+}$ dimers. In recent work on HMC-22 based catalysts using ammonium heptamolybdate as a molybdenum source, Ma et al. [34] have proposed that monomeric oxomolybdenum species are of importance. On the basis of the results reported here, it is not possible to further postulate the form of the active precursor. Studies with the

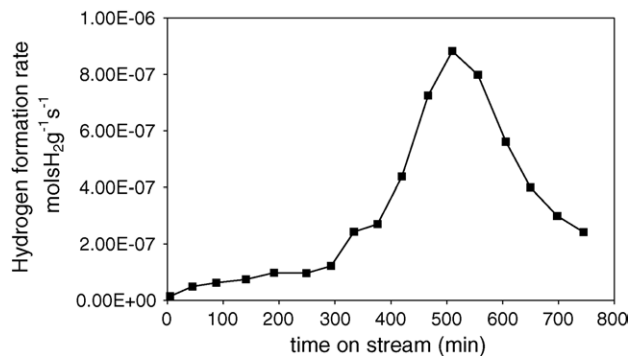


Fig. 5. Hydrogen production of 5 wt.% P/5 wt.% $\text{MoO}_3/\text{ZSM-5}$ as a function of time on stream.

catalysts prepared from both ammonium heptamolybdate and phosphomolybdic acid demonstrate that there is no influence of pre-calcination on reaction performance, implying that the form of the oxomolybdenum species prior to exposure to the reaction environment may not be all that significant.

In view of the relatively large effect of phosphorus in relation to its concentration apparent in Fig. 3, the influence of much higher levels of phosphorus addition was investigated. Fig. 5 presents the results for a 5 wt.% P/5 wt.% $\text{MoO}_3/\text{ZSM-5}$ catalyst. At this level of phosphorus addition, the overall conversion was suppressed. Moreover, the production of benzene was entirely eliminated. It was observed, however, that there was a very low level of hydrogen production, which was found to increase initially gradually with time on line. At longer run times the rate of increase of formation was found to pass through a maximum, corresponding to $>5\%$ of the exit product stream at ca. 510 min on stream. The on-set of this maximum was associated with the evolution of a pungent-smelling orange deposit from the catalyst which subsequent ^{31}P NMR analysis showed to be a phosphite. Furthermore the absence of any signals in the ^{13}C NMR spectrum confirmed it to be an inorganic phosphite. Off-line gas-phase FT-IR analysis of the effluent suggested that only traces of carbon oxides were formed during reaction. Beyond the maximum, traces of benzene and higher hydrocarbons could be evidenced in the gc analysis, but they were present in concentrations estimated to be $<0.02\%$. This observation is interesting in view of the fact that it could possibly be a CO-free route to hydrogen. However the reaction rate is very low and it is important to understand the processes leading to the activity pattern. The inclusion of molybdenum was found to be crucial for this behaviour since phosphorus modified ZSM-5 did not have any detectable activity for hydrogen production. However, 5% P doped bulk MoO_3 was investigated and the results are shown in Fig. 6. In terms of hydrogen production, the overall activity pattern with time on stream appears similar to that reported in Fig. 5, which could imply a similarity in formation route. In contrast to the zeolite system, the burst in H_2 formation rate was found to be associated with simultaneous bursts for CO and CO_2 as determined by off-line FT-IR analysis of the reactor effluent gas. Furthermore, there was no evolution of an inorganic phosphite phase with this system. In the case of the zeolite system, there was no evidence for any phase other than ZSM-5 in the XRD

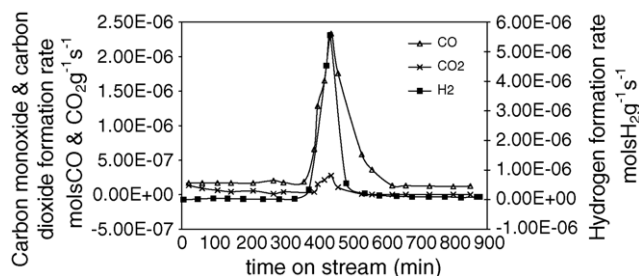


Fig. 6. Products formed from the isothermal carburisation of 5% P/MoO₃ at the reaction conditions employed in Fig. 5.

pattern of the post-reaction material, implying that any molybdenum and/or phosphorus containing phases were either highly dispersed and/or amorphous. However, post-reaction XRD of the bulk P/MoO₃ material yielded the pattern presented in Fig. 7. This pattern can be indexed to a mixture of molybdenum phosphide and eta-molybdenum carbide phases. This implies that the evolution of hydrogen and carbon oxides is associated with the carbiding of the MoO₃ component, although the carbide formed is not the usual β -Mo₂C phase, which is expected [35]. Within the literature, there appears to have been very few studies of the isothermal carbiding of MoO₃ with methane, most studies have followed the process using temperature programmed routes with H₂/CH₄ mixtures, e.g. [23,36,37]. However, very recently Lacheen and Iglesia [33] have investigated the isothermal activation pathways of oxomolybdenum species in ZSM-5 using pure methane at a temperature of ca. 680 °C. In general terms, relative concentrations and times of evolution of H₂, CO and CO₂ observed are strikingly similar to those evident in Fig. 6. However, with their studies the maxima were obtained after ca. 10 min on-stream, in contrast to the ca. 7.5 h observed in Fig. 6. This starkly illustrates the massive enhancement of carbiding

rate observed on dispersion of MoO₃ on the ZSM-5 matrix, since experiments showed that although the inclusion of phosphorus did delay the carbiding process, it was by ca. 85 min under the conditions used in Fig. 6. The nature of the phase transition with time on stream reported in Fig. 6 is consistent with reports that the isothermal reduction of the bulk MoO₃ phase involves an induction period which has been ascribed to rate-determining nucleation or autocatalytic effects [38]. Lacheen and Iglesia [33] have reported that the carburisation process in methane aromatisation catalysts is autocatalytic, with intermediate olefins being formed which enhance the rate of carburisation.

In view of the similarity of the general “burst” of hydrogen between the 5% P/5% MoO₃/ZSM-5 and 5%P/MoO₃ it is tempting to ascribe its formation as being due to carbiding in the former case. The lack concomitant carbon oxides cast doubt on this suggestion. Another aspect which requires consideration is the evolution of the phosphite phase. Its formation necessitates the reduction of phosphate which would lead to an oxidised product. Whilst this may be water, for which the analytical set-up is not optimised, the alternative of an oxidation product being formed by, e.g., a Mars–van Krevelen type process which has not been detected cannot be discounted. In this context it is of relevance that the addition of phosphorus to MoO₃ has been reported to enhance its performance in the oxidative dehydrogenation of propane [39]. This reaction is believed to occur via a Mars–van Krevelen mechanism. Post-reaction CHN analysis of the zeolite based sample is reported in Table 1 and it is apparent that the overall carbon content is close to that which would be expected where the Mo₂C phase formed. However, that is not to say that it is formed and this requires further elucidation possibly using EXAFS. Ammonia TPD experiments, aimed at understanding the effect of phosphorus addition on the acidity of 5% P/5% MoO₃/ZSM-5, are currently in progress.

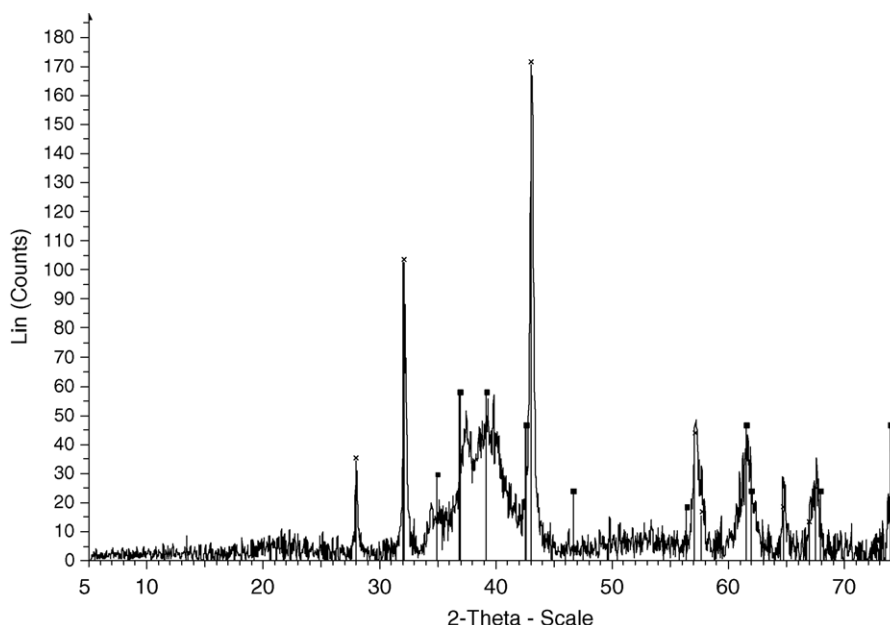


Fig. 7. XRD pattern of 5% P/MoO₃ following carburisation × MoP ■ eta-MoC.

4. Conclusion

The influence of phosphorus doping on the methane dehydroaromatisation activity of MoO₃/ZSM-5 catalysts has been investigated. Preparation of catalysts with phosphomolybdic acid is observed to reduce the overall activity with respect to counterparts prepared using ammonium heptamolybdate. In particular the use of phosphomolybdic acid increases the observed hydrogen to benzene ratio, which is explained on the basis of enhanced coking. No evidence for discrete MoO₃ phases could be found in both catalyst precursors by Raman spectroscopy and the possible production of the β-MoO₃ phase, which may be expected on the basis of literature reports on the thermal decomposition of phosphomolybdic acid, can be ruled out. When the ammonium molybdate catalyst is doped with 5 wt.% phosphorus from an ammonium dihydrogen phosphate precursor, hydrocarbon production is suppressed and hydrogen is the sole gas-phase product observed. Although the hydrogen formation rate is low, it increases with time reaching a maximum after ca. 510 min which corresponds to >5% of the exit stream concentration. The appearance of this maximum is associated with the evolution of an inorganic phosphite phase from the catalyst. The decline of hydrogen formation rate beyond the maximum is associated with the production of trace levels of benzene (<0.02%). Studies of bulk MoO₃ and bulk 5 wt.% P/MoO₃ have shown that the hydrogen evolution pattern is qualitatively similar. However in these cases, CO and CO₂ maxima are obtained simultaneously with the H₂ maximum, and the relative ratios of the products are similar to recent reports of the carburization of oxomolybdenum ZSM-5 catalysts, although the timescales are much greater. It is tempting to ascribe the behaviour of the 5 wt.% P/5 wt.% MoO₃/ZSM-5 to carburisation of the oxomolybdenum component but the absence of gas-phase carbon oxides would be surprising unless they were retained on the catalyst in some form. Post-reaction CHN analysis is consistent with the formation of the carbide, but further studies are required to elucidate this.

Acknowledgements

We are grateful to the EPSRC and the Department of Chemistry, University of Glasgow, for the award of a DTA studentship (to SB) and to the Royal Society and DST for the award of India–UK network grants to JSJH and KMP and JSJH and PP. We thank Mrs. Kim Wilson, University of Glasgow, for kind assistance with CHN analyses and Dr. David Rycroft, University of Glasgow, for kindly recording and interpreting NMR spectra. Professor Ewen Smith and Dr. Ann Robin, University of Strathclyde are gratefully acknowledged for their generous help with the Raman experiments.

References

[1] Y. Xu, X. Bao, L. Lin, *J. Catal.* 216 (2003) 386.

- [2] T.V. Choudhary, E. Aksoylu, D.W. Goodman, *Catal. Rev.* 45 (2003) 151.
- [3] G.J. Hutchings, M.S. Scurrell, J.R. Woodhouse, *Chem. Soc. Rev.* 18 (1989) 251.
- [4] T.J. Hall, J.S.J. Hargreaves, G.J. Hutchings, R.W. Joyner, S.H. Taylor, *Fuel Proc. Technol.* 42 (1995) 151.
- [5] M. Belgued, P. Pareja, A. Amariglio, H. Amariglio, *Nature* 352 (1991) 789.
- [6] T. Koerts, R.A. van Santen, *J. Chem. Soc., Chem. Commun.* (1991) 1281.
- [7] L. Wang, L. Tao, M. Xie, G. Xu, J. Huang, Y. Xu, *Catal. Lett.* 21 (1993) 35.
- [8] Y. Shu, Y. Xu, S. Wong, L. Wang, X. Guo, *J. Catal.* 170 (1997) 11.
- [9] S. Liu, Q. Dong, R. Ohnishi, M. Ichikawa, *Chem. Commun.* (1997) 1455.
- [10] R. Ohnishi, S. Liu, Q. Dong, L. Wang, M. Ichikawa, *J. Catal.* 182 (1999) 92.
- [11] Y. Shu, R. Ohnishi, M. Ichikawa, *J. Catal.* 206 (2002) 134.
- [12] H.S. Lacheen, E. Iglesia, *J. Catal.* 230 (2005) 173.
- [13] D. Wang, J.H. Lunsford, M.P. Rosynek, *J. Catal.* 169 (1997) 347.
- [14] J.-Z. Zhang, M.A. Long, R.F. Howe, *Catal. Today* 44 (1998) 293.
- [15] F. Solymosi, A. Szoke, J. Cserenyi, *Catal. Lett.* 39 (1996) 157.
- [16] S.B. Derouane-Abd. Hamid, J.R. Anderson, I. Schmidt, C. Bouchy, C.J.H. Jacobsen, E.G. Derouane, *Catal. Today* 63 (2000) 461.
- [17] C. Bouchy, I. Schmidt, J.R. Anderson, C.J.H. Jacobsen, E.G. Derouane, S.B. Derouane-Abd. Hamid, *J. Mol. Catal. A: Chem.* 163 (2000) 283.
- [18] F. Solymosi, J. Cserenyi, A. Szoke, T. Bansagi, A. Ozko, *J. Catal.* 165 (1997) 510.
- [19] V.T.T. Ha, L.V. Tiep, P. Meriaudeau, C. Naccache, *J. Mol. Catal. A: Chem.* 181 (2002) 283.
- [20] Y. Shu, D. Ma, X. Bao, X. Lu, *Catal. Lett.* 66 (2000) 161.
- [21] Y. Shu, D. Ma, X. Liu, X. Han, Y. Xu, X. Bao, *J. Phys. Chem. B* 104 (2000) 8245.
- [22] L. Chen, L. Lin, Z. Xu, X. Li, T. Zhang, *J. Catal.* 157 (1995) 190.
- [23] P. Perez-Romo, C. Potvin, J.-M. Manoli, M.M. Chehimi, G. Djegamariadassou, *J. Catal.* 208 (2002) 187.
- [24] T. Zhang, M. Amiridis, *Appl. Catal. A: Gen.* 167 (1998) 161.
- [25] R. Aiello, J. Fiscus, H. Loye, M. Amiridis, *Appl. Catal. A: Gen.* 192 (2000) 227.
- [26] R.A. Couttenye, M.H. De Vila, S.L. Suib, *J. Catal.* 233 (2005) 317.
- [27] M. Ai, *Polyhedron* 5 (1986) 103.
- [28] H. de Lasa, L. Hagey, S. Rong, A. Pekediz, *Chem. Eng. Sci.* 51 (1996) 2885.
- [29] M. Fournier, A. Aouissi, C. Rocchiccioli-Deltcheff, *J. Chem. Soc., Chem. Commun.* (1994) 307.
- [30] I.R. Beattie, T.R. Gilson, *J. Chem. Soc. A* (1969) 2322.
- [31] E.M. McCarron III, *J. Chem. Soc., Chem. Commun.* (1986) 336.
- [32] R.W. Li, G.D. Meitzner, R.W. Borry III, E. Iglesia, *J. Catal.* 191 (2000) 373.
- [33] H.S. Lacheen, E. Iglesia, *Phys. Chem. Chem. Phys.* 7 (2005) 538.
- [34] D. Ma, Q. Zhu, D. Zhou, Y. Shu, Y. Xu, X. Bao, *Phys. Chem. Chem. Phys.* 7 (2005) 3102.
- [35] J.-G. Choi, J.R. Brenner, L.T. Thompson, *J. Catal.* 154 (1995) 33.
- [36] K.T. Jung, W.B. Kim, C.H. Rhee, J.S. Lee, *Chem. Mater.* 16 (2004) 307.
- [37] T. Xiao, A.P.E. York, K.S. Coleman, J.B. Claridge, J. Sloan, J. Charnock, M.L.H. Green, *J. Mater. Chem.* 11 (2001) 3094.
- [38] P. Arnoldy, J.C.M. de Jonge, J.A. Moulijn, *J. Phys. Chem.* 89 (1985) 4517.
- [39] X. Zhang, H. Lin, W. Wang, X. Yi, *Appl. Surf. Sci.* 220 (2003) 117.